Theor Chem Account (2007) 118:541–547
DOI 10.1007/s00214-007-0338-y

REGULAR ARTICLE

Order-*N* and embedded-cluster first-principles DFT calculations using SIESTA/Mosaico

Luis Seijo · Zoila Barandiarán · José M. Soler

Received: 21 December 2006 / Accepted: 13 March 2007 / Published online: 6 June 2007
© Springer-Verlag 2007

Abstract Order-*N* and embedded-cluster first-principles DFT calculations have been performed with the Mosaico method for energy optimization (Seijo and Barandiarán in J Chem Phys **121**:6698, 2004) for the first time. The Hamiltonian matrix elements have been computed with the SIESTA code. The order-*N* behavior of the method in DFT calculations was shown in total energy calculations performed on bulk silicon using supercells up to Si_{8000}. The sizes of the orbital-specific-basis-sets needed for precise calculations have been explored in demanding (bulk silicon) and favorable (water clusters) cases for a method based on the calculation of localized molecular orbitals. Embedded-cluster calculations, which are much faster than full-system calculations, have been performed on an Si-vacancy of bulk silicon and on a water cluster with a displacing water molecule. The feasiability of calculations of this type with Mosaico has been demonstrated. The sizes of the variationally free, active clusters which are needed for an agreement with full-system calculations have been explored and result to be reasonably small.

Contribution to the Serafin Fraga Memorial Issue.

L. Seijo (✉) · Z. Barandiarán
Departamento de Química, C-XIV,
Universidad Autónoma de Madrid, 28049 Madrid, Spain
e-mail: luis.seijo@uam.es

L. Seijo · Z. Barandiarán · J. M. Soler
Instituto Universitario de Ciencia de Materiales Nicolás Cabrera,
Universidad Autónoma de Madrid, 28049 Madrid, Spain

J. M. Soler
Departamento de Física de la Materia Condensada, C-III,
Universidad Autónoma de Madrid, 28049 Madrid, Spain

1 Introduction

In [1], the Mosaico method was presented for linear-scaling energy minimization in semiempirical and first-principles Hartree–Fock and Kohn–Sham electronic structure calculations on molecules and solids. It belongs to the family of methods that handle the energy minimization step in a way that scales in low order with the size of the molecule or, more precisely, with the basis set size [2–10] (see [11] and [12] for review). Mosaico exploits the self-consistent or on-the-fly calculation of the localized molecular orbitals (LMO) of a localization method of choice (instead of the usual self-consistent calculation of the canonical orbitals followed by an after-the-fly localization). The set of LMOs (or mosaic) is divided in subsets (or *tesserae*); the LMOs of a *tessera* are the solutions of an embedded-cluster like pseudoeigenvalue equation which is solved in a linear expansion approximation using a basis set specific for the *tessera*; the set of coupled embedded-*tessera* equations is solved self-consistently. This procedure is parallel by construction. Moreover, after calculating a large molecule, a new molecule which resulted from creating a chemical defect on the old one, could be calculated in an embedded-cluster type of approach by freezing most of the *tesserae* while letting variationally free a few of them around the chemical defect [1].

Since Mosaico is expected to be useful in calculations of very large molecules, it must be used together with fast methods for the computation of the Hamiltonian matrix. Up to now [1], it had only been used together with the inexpensive semiempirical extended Hückel Hamiltonian [13]. In this paper, the Mosaico method has been implemented together with the SIESTA method [14,15] for self-consistent DFT calculations. SIESTA makes use of standard core pseudopotentials and linear combination of numerical atomic orbitals in local density and generalized gradient DFT approximations;

projecting the atomic orbitals and the density in a real-space grid, SIESTA computes the Kohn–Sham Hamiltonian with a number of operations that scales linearly with the size of the system. We present results of Γ-point total energy DFT calculations in bulk-Si using supercells up to Si_{8000}, as well as in water clusters. The potentialities of the embedded-cluster approach are shown with embedded-cluster calculations performed on an Si-vacancy in bulk-Si and in a water molecule moving across a water cluster.

2 Method

In a standard molecular calculation performed with local basis sets (like Gaussian-type functions, numerical atomic orbitals, etc.), all the molecular orbitals (MO) are expressed as linear combinations of a common set of b_{MOL} basis set functions, which is the molecular basis set:

$$\underline{\chi} = \left(|\,\chi_1\rangle, |\,\chi_2\rangle, \ldots, |\,\chi_{b_{MOL}}\rangle\right) . \tag{1}$$

Instead, in the Mosaico method we work with orbital-specific-basis-sets (OSBS) [1]. We are aimed at computing the localized MOs (LMO) of a given localization method (such as the popular methods of Boys [16], Edmiston and Ruedenberg [17], and Pipek and Mezey [18], or the projected-localized MO method, PLMO, [19,1]) and the LMOs localized in a region of real space are arbitrarily grouped together in what is called a *tessera* (one of the little tiles of which mosaics are made) and forced to be expressed as linear combinations of a subset of the molecular basis set, which we call as the *tessera*-basis-set or orbital-specific-basis-set. For instance, the basis set of a given *tessera*, let us say *tessera-A*, reads

$$\underline{\chi}_A = \left(|\,\chi_{A1}\rangle, |\,\chi_{A2}\rangle, \ldots, |\,\chi_{Ab_A}\rangle\right) \tag{2}$$

and is made of b_A functions of $\underline{\chi}$ (Eq. 1). The basis sets of all other *tesserae*, B, C, ..., are chosen similarly and, usually, in such a way that several *tesserae* share a number of basis set functions.

The working equations of the Mosaico method are the embedded-*tessera* equations. The equation for *tessera A* reads

$$\underline{F}^L_A \, \underline{C}^L_A = \underline{S}^L_A \, \underline{C}^L_A \, \underline{\lambda}_A . \tag{3}$$

In Eq. 3, $\underline{C}^L_A$ is the $b_A \times n_A$ coefficient matrix of n_A occupied LMOs of *tessera-A*,

$$\underline{\varphi}^L_A = \underline{\chi}_A \, \underline{C}^L_A , \tag{4}$$

and $\underline{F}^L_A$ and $\underline{S}_A$ are the $b_A \times b_A$ matrix representations of the effective Fock or Kohn–Sham operator of the embedded *tessera-A*, $\hat{F}^L_A$, and the unit operator in the $\underline{\chi}_A$ basis set,

$$\underline{F}^L_A = \underline{\chi}^\dagger_A \, \hat{F}^L_A \, \underline{\chi}_A , \quad \underline{S}^L_A = \underline{\chi}^\dagger_A \, \underline{\chi}_A , \tag{5}$$

with

$$\hat{F}^L_A \equiv \hat{F} - \hat{\rho}\,\hat{F}\,\hat{\rho} + \hat{\rho}\,\hat{L}_A\,\hat{\rho}, \tag{6}$$

$\hat{F}$ being the Fock or Kohn–Sham operator of the whole system, $\hat{\rho}$ the density operator and $\hat{L}_A$ the localization operator on *tessera-A*. When the explicit form of $\hat{L}_A$ is unknown for a localization method, a practical definition of it is its spectral representation

$$\hat{L}_A = \underline{\varphi}^L_A \, \underline{\lambda}_A \, \underline{\varphi}^{L\dagger}_A , \quad \underline{\varphi}^L_A = \underline{\varphi}^{(0)} \, {}_0\underline{U}^{L(A)} , \tag{7}$$

where $\underline{\lambda}_A$ is a $n_A \times n_A$ diagonal matrix of arbitrary negative numbers; at a given iteration toward convergence, $\underline{\varphi}^L_A$ are n_A of the n LMOs obtained after applying the localization method of choice to the LMOs of the previous iteration, $\underline{\varphi}^{(0)}$ (${}_0\underline{U}^{L(A)}$ is a rectangular matrix made of the n_A columns of the unitary localization matrix resulting from the localization procedure); at convergence, the $\underline{\varphi}^L_A$ LMOs are the solutions of Eq. 3 (Eq. 4).

Standard explicit localizations have high order dependencies on the total number of occupied MOs, n. However, in Mosaico, the explicit localization procedure is applied to a set of localized MOs, not to the set of canonical delocalized MOs; this fact allows us to perform the localization by means of local rotations or, in other words, by computing the LMOs of one *tessera* out of a unitary transformation involving only LMOs of neighbor *tesserae*.

The procedure for a complete SIESTA/Mosaico DFT calculation is the following. (1) Make an initial guess for the density matrix. (2) Compute the matrix of the Kohn–Sham operator of the system on the molecular basis set, which is sparse. (3) Enter the Mosaico procedure, which is: (3a) Start with an initial guess of LMOs. (3b) For all *tesserae*, apply the chosen localization method (with local rotations) and compute Eq. 7. (3c) For all *tesserae*, compute Eq. 5 and solve Eq. 3. (3d) Check convergence of the LMOs: The initial LMOs, the LMOs after explicit localization (Eq. 7), and the LMOs after the embedded-*tesserae* equations (Eqs. 3 and 4) should coincide within given precision. Go to (3b) if convergence has not been reached. (3e) Compute the density matrix and exit the Mosaico procedure. (4) Check convergence of the density matrix; go to (2) if convergence has not been reached.

The calculation of the sparse matrix of the Kohn–Sham operator of the system on the molecular basis set is done in a linear-scaling fashion according to the standard procedures of SIESTA [15]. Exchange and correlation are treated in the local density approximation (LDA). Core electrons are

substituted by norm conserving pseudopotentials [20] in their fully nonlocal form [21]. A minimal basis set of strictly localized atomic orbitals [22] was used for valence electrons. Their spatial range was fixed by an energy shift parameter [15] of 0.3 eV.

The solutions of the embedded-*tessera* equations (Eq. 3), which span the same optimal occupied orbital space as the canonical solutions of the Hartree–Fock or the Kohn–Sham equations, are n orthogonal LMOs of the localization method of choice, in principle. It is also in practice for choices of *tessera*-basis-sets sufficiently large. Often, the *tessera*-basis-sets will not be so large and residual nonorthogonality between the LMOs of different *tesserae* will be observed as a consequence. In this case, a proper calculation of total energies requires to use the correct density matrix for nonorthogonal orbitals, defined as

$$\underline{D} = \underline{C}^{L}\,\underline{S}^{-1}\,\underline{C}^{L\dagger}, \tag{8}$$

where $\underline{C}^{L}$ is the coefficient matrix of all occupied LMOs and $\underline{S}$ the overlap matrix between them. In order to avoid the high-order inversion of $\underline{S}$, we will use a truncated Taylor series expansion of $\underline{S}^{-1}$,

$$\underline{S}^{-1} \approx \sum_{j=0}^{m} \left(\underline{1} - \underline{S}\right)^{j}, \tag{9}$$

and call $\underline{D}^{(m)}$ and $E^{(m)}$ the corresponding approximated density matrix and total energy.

Finally, if we want to compute the electronic structure of a big molecule that can be seen as resulting from the creation of a chemical defect on another big molecule we computed before, we could choose not to perform a full-system calculation but, instead, a simpler embedded-cluster calculation. In this case, in Mosaico we can define the embedded-cluster as a set of several embedded-*tesserae*, and the embedded-cluster calculation is performed just skeeping all frozen *tesserae* in steps (3b) and (3c). This kind of calculation is in the spirit of those proposed by Ordejon et al [23] for the linear scaling phonon calculations.

3 Results

3.1 Bulk silicon

We have done Γ-point total energy calculations of bulk silicon (diamond structure, $a = 5.43$ Å) with several supercell sizes at the single-zeta (SZ) basis set level. Although the SZ calculations are not sufficient for chemical studies, they are good to check the possibility of doing first-principles DFT calculations with Mosaico, which is the ultimate aim of this paper. The small band gap of silicon makes the calculation very demanding for a method like Mosaico whose performance depends on the degree of localization achieved. In effect, small gaps make the maximum achievable localization very small, so that we may expect to need *tessera*-basis-sets which extend very far away from the atoms where the LMOs are expected to have their maximum values.

The localization method chosen here was the PLMO method [1,19], for its simplicity. The PLMO method gives the LMOs that maximize overlap with a set of reference orbitals. For the reference, we have chosen a very simple set: the sums of the two sp^3 hybrid AOs of every couple of neigbhor Si atoms pointing toward each other.

The *tesserae* have been defined as sets of four LMOs surrounding every other Si atom (or, more precisely, the four LMOs with higher overlap with the four reference orbitals attached to the Si atom).

Several *tesserae*-basis-sets have been used, called 1N, 2N, 3N, and 4N. In them, the four LMOs of a *tessera* have been expressed as linear combinations of the following AOs: (1N) The AOs of the five Si atoms involved in the four sigma bonds (a central Si atom and its four neigbhors), plus AOs of their 12 first neighbors; so, 17 atoms are contributing their AOs to the LMOs, which, at the SZ level, means 68 basis set functions per *tessera*. (2N) The AOs of the next-neighbor Si atoms are also included, which means AOs of a total of 41 atoms and 164 basis set functions per *tessera*. (3N) and (4N) are made in the same manner, with AOs of 83 atoms and 147 atoms per *tessera*, respectively.

The results are summarized in Figs. 1, 2, 3. The cohesive energy per Si atom of bulk silicon, as resulting from Γ-point total energy calculations on the Si_{512} supercell, deviates from the canonical calculation as shown in Fig. 1. The errors diminish with the *tessera*-basis-set size, as expected. They remain

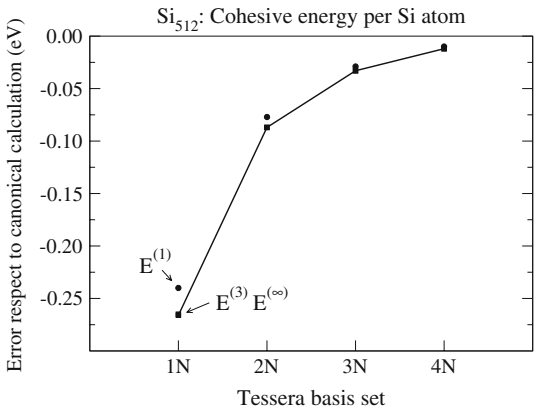

Fig. 1 Γ-point total energy calculations on the Si_{512} supercell: deviations from the canonical calculation of the cohesive energy of bulk silicon per Si atom as a function of the *tessera*-basis-set size (see text for definitions of *tessera*-basis-sets 1N, 2N, 3N, and 4N). $E^{(m)}$ means that the density matrix has been calculated with an m-order Taylor series expansion of the reciprocal overlap matrix of the LMOs

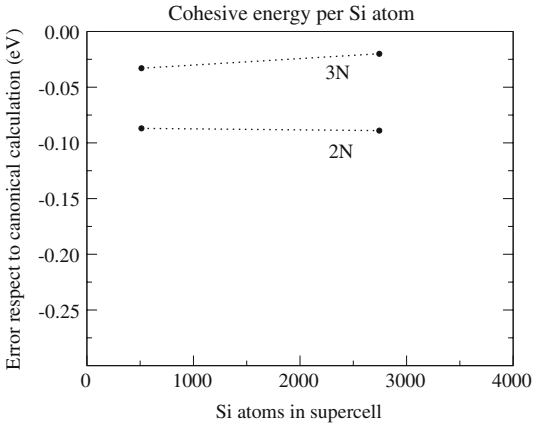

Fig. 2 Deviations from the canonical calculation of the cohesive energy of bulk silicon per Si atom as a function of the supercell size. 2N and 3N *tessera*-basis-set results are shown

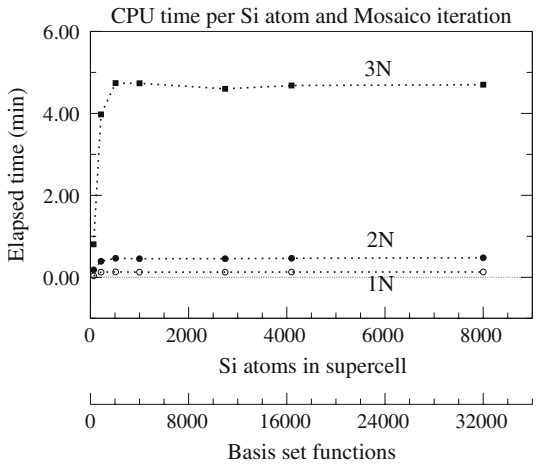

Fig. 3 Elapsed time per Si atom and Mosaico iteration as a function of the supercell size used in the calculation of bulk silicon

nonnegligible even at the 4N level as a consequence of the relatively low degree of localization that can be achieved in this material because of its low band gap, which is what makes this material a hard test for the Mosaico method. The errors at the 2N and 3N levels are quite acceptable. As we can see in the figure, the residual nonorthogonality of the LMOs diminish when the basis set is improved, as shown by the difference between the energy calculated with a density matrix approximated with a first-order Taylor expansion of $\underline{S}^{-1}$, $E^{(1)}$, and the true energy, $E^{(\infty)}$. A third-order expansion of $\underline{S}^{-1}$ is sufficient to make the approximate and the true energies indistinguishable in the figure. Fig. 2 shows that the errors computed in Si_{512} are basically independent of the supercell size and can be extended to other supercell sizes.

Finally, Fig. 3 shows the elapsed computer times per Si atom. The times correspond to one Mosaico iteration (steps 3b and 3c) performed in a single processor desktop PC. The number of Mosaico iterations necessary for convergence in this inner self-consistency loop varies along the outer, standard self-consistent field (scf) iterations of the density matrix (loop (2)). At the beginning of the scf procedure, around 20 Mosaico iterations would be necessary; however, there is no point in trying to achieve full Mosaico convergence with a Hamiltonian that is not the final one and, in consequence, loop (3) is exited after 10 Mosaico iterations. After a few scf iterations of the density matrix, around five Mosaico iterations are sufficient for convergence. Obviously, when the scf process is about to convergence, only one Mosaico iteration is needed. We have not observed significant differences between the number of scf iterations needed for convergence when Mosaico and when standard diagonalization was used. An estimate of the elapsed time required for the diagonalization in the Si_{8000} case, out of the times in Si_{216} and Si_{512} in similar conditions, gives around 120 s per Si atom; this means that the present implementation of the Mosaico procedure still needs significant improvements in order to be competitive.

We must note that the calculation of each one of the 4000 *tesserae* of Si_{8000}, for instance, was performed without using any information produced in the calculation of other *tesserae* in the same Mosaico iteration, so that they can be split in 4000 independent single-*tessera* calculations performed in parallel. Figure 3 shows the linear-scaling feature of Mosaico. The scaling slope, which is the height of the lines in Fig. 3, scales as the cube of the single-*tessera* basis set size, as it corresponds to the diagonalization involved in Eq. 3.

3.2 Si-vacancy

The Mosaico procedure converges to a particular set of LMOs giving the optimum density matrix, rather than to any set of LMOs giving the optimum density matrix. This feature might help reaching convergence in difficult cases like the recombination of dangling bonds. Another feature of Mosaico is its ability to be used as an embedded-cluster method straightforwardly, just by freezing most of the *tesserae* previously computed in a similar system and relaxing only a few active *tesserae*, which could mean important savings in series of calculations of similar systems. Here, the formation energy of an Si-vacancy in bulk silicon was calculated in order to show the two features.

The details of the calculation were the same as in Sect. 3.1. At this level of calculation, the formation energy of the Si-vacancy calculated with an Si_{216} supercell and neglecting lattice relaxation is 6.18 eV, higher than the experimental value of 3.6 eV. Although lattice relaxation and a better basis set would be required for a better calculation of the vacancy formation energy, the simpler level of the present calculation

Table 1 Embedded-cluster calculations of the formation energy of an Si-vacancy in bulk silicon

Embedded cluster	# *Tesserae*	# LMOs	Formation energy (eV)
Two recombined bonds	1	2	8.8
+ 12 × 4σ bonds	13	50	6.3
+ 56 × 4σ bonds	69	274	6.18

The results correspond to 2N *tessera*-basis-set calculations on a Si_{216} supercell, using an $E^{(3)}$ approximation. The canonical result on the full system is 6.18 eV

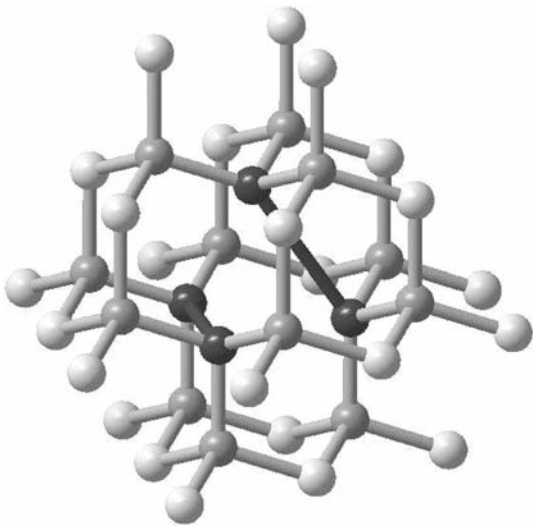

Fig. 4 Schematic representation of the Si-vacancy of bulk silicon

is sufficient for the declared goals. The results are summarized in Table 1.

Firstly, all embedded-cluster calculations done in Si_{216} : V_{Si} converged smoothly. In the simplest one, all the LMOs except the two that will result from the recombination of the four unpaired electrons created by the vacancy were taken from a previous calculation on the Si_{216} supercell of bulk silicon and frozen. In this calculation, only one *tessera* of two LMOs was variationally relaxed (schematically represented by the darkest sticks in Fig. 4) and the resulting formation energy was 8.8 eV. Additional variational relaxation of 48 LMOs grouped in the 12 *tesserae* next to the two recombined bonds (schematically represented by the clearer sticks in Fig. 4) gave 6.3 eV, which is very close to the 6.18 eV limit. This limit was reached when the LMOs of the next 56 surrounding *tesserae* were included. The convergence of the formation energy with the cluster size observed in the Si_{216} supercell should be the same for larger supercells; in them, the CPU savings with respect to a full-system calculation would be comparatively much larger.

3.3 Water clusters

We have seen the linear-scaling feature of Mosaico with the DFT calculations on bulk silicon using several supercell sizes. Bulk silicon was a very demanding system for Mosaico because of the low gap and the relatively low degree of localization achievable, and quite large *tessera*-basis-sets were required for a high precision in the computed energies. One could expect other systems not to be so demanding in terms of *tessera*-basis-sets; one example could be water clusters. In order to check the *tessera*-basis-set requirements for high precision in a not so demanding system, we have performed SIESTA/Mosaico DFT calculations in a $(H_2O)_{98}$ cluster, whose geometry corresponds to a roughly spherical portion in a snapshot of an *ab initio* molecular dynamics simulation of bulk liquid water [24]. Thus, it contains all kinds of deformations of the water molecules. We have also checked the performance of the embedded-cluster approximation in clusters that resulted from the original one by shifting one single water molecule along an arbitrary axis.

As before, we used an SZ basis set and the PLMO localization method; as a set of reference orbitals we used $2s(\mathrm{O}) + 1s(H_1)$, $2s(\mathrm{O}) + 1s(H_2)$, $2p_\perp(\mathrm{O}) + 2p_\parallel(\mathrm{O})$, and $2p_\perp(\mathrm{O}) - 2p_\parallel(\mathrm{O})$ for each water molecule, where $2p_\perp(\mathrm{O})$ and $2p_\parallel(\mathrm{O})$ are the linear combinations of oxygen $2p$ AOs which are perpendicular to the molecular plane and parallel to it, the latter one bisecting the molecular angle. The *tesserae* have been defined as sets of four LMOs localized on each water molecule (one *tessera* is made of the four LMOs of higher overlap with the four reference orbitals of a water molecule).

In Fig. 5, we show the precision of the total energy as a function of the size of the *tessera*-basis-set used. Each water molecule is calculated with a basis set made of AOs of all

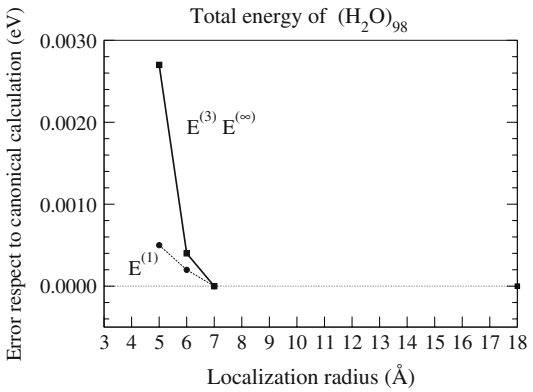

Fig. 5 Deviations from the canonical calculation of the total energy of a $(H_2O)_{98}$ cluster as a function of the *tessera*-basis-set size. The basis set used for each water molecule contains AOs of all water molecules within the localization radius. $E^{(m)}$ means that the density matrix has been calculated with an m-order Taylor series expansion of the reciprocal overlap matrix of the LMOs

water molecules within a given radius, called the localization radius. We see that a full practical precision is achieved with a localization radius of 7 Å, which contains AOs of 26.4 water molecules in average. Clearly, this is a more favorable case than bulk silicon. Besides, as in bulk silicon, a third-order Taylor expansion of the reciprocal overlap matrix between the LMOs is sufficient for a correct calculation of the total energy with all *tessera*-basis-sets explored. With the 7 Å localization radius, however, the computed LMOs are practically orthogonal and a first-order Taylor expansion is sufficient (and even unnecessary).

In Fig. 6, we show the total energy curves corresponding to shifting one water molecule, arbitrarily chosen, along an arbitrary z-axis. The full-line is the canonical result and serves as a reference of quality for the calculations performed within the embedded-cluster approximation, which are the other lines. The number of water molecules whose LMOs are frozen and whose LMOs are optimized in the respective embedded-cluster approximation are indicated in the figure. The LMOs of the variationally relaxed water molecules are calculated with a basis set made of all AOs on the water molecules within a radius of 7 Å. As we see, electronic

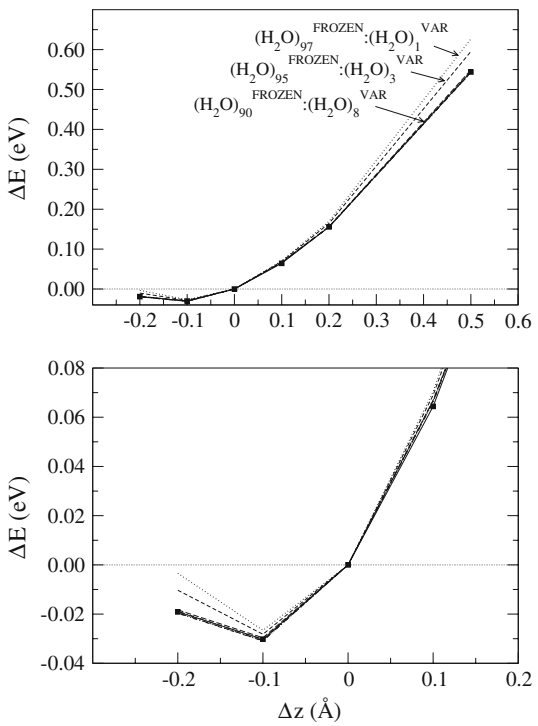

Fig. 6 Embedded-cluster calculations of the total energy change of a $(H_2O)_{98}$ cluster due to the translation Δz of one water molecule along an arbitrary axis. Reference energy is −45229.0224 eV. *Full line* Canonical calculation on the full-system. *Other lines* The numbers of water molecules whose electronic structure was frozen or variationally relaxed are indicated in the *upper panel*. The region of the minimum is zoomed in the *lower panel*, where the *lines* corresponding to 17 and 29 variational water molecules are also shown

relaxation of one single water molecule already gives quite good results, specially for small displacements. Relaxing a total of three water molecules improves slightly the result and relaxing eight (the shifted one and the closest seven) leads to the canonical result in practical terms. We may remark that restricting the number of variational molecules leads to larger curvatures; this behavior is in agreement with the phonon stiffening in diamond observed by Ordejon et al [23] as a consequence of the restriction in the variational freedom.

4 Conclusions

In this paper, we have performed order-N and embedded-cluster first-principles DFT calculations with the Mosaico method for energy optimization [1] for the first time. The Hamiltonian matrix elements have been computed with the SIESTA code [14,15]. The order-N behavior of the method in DFT calculations was shown in bulk silicon calculated using supercells up to Si_{8000}. The sizes of the orbital-specific-basis-sets needed for precise calculations have been explored in the demanding case of bulk silicon and in the more favorable case of water clusters.

Embedded-cluster calculations, which are much faster than full-system calculations, have been performed on an Si-vacancy of bulk silicon and on a water cluster with a displacing water molecule, taking advantage of previously performed full-system calculations on bulk silicon and on an original water cluster, respectively. The feasiability of this type of convenient calculations with Mosaico has been demonstrated. The sizes of the variationally free, active clusters which are needed for an agreement with full-system calculations have been explored and result to be reasonably small.

Acknowledgments This work was partly supported by grants CTQ2005-08550 and FIS2006-12117 from Ministerio de Educación y Ciencia, Spain (Dirección General de Investigación). We are grateful to Prof. E. Artacho, University of Cambridge, for helpful discussions and suggestions, to M. V. Fernandez-Serra for providing us snapshots of first-principles molecular dynamics simulations of liquid water, and to S. S. Alexandre for helping us with pseudopotential generation.

References

1. Seijo L, Barandiarán Z (2004) J Chem Phys 121:6698
2. Yang W (1991) Phys Rev Lett 66:1438
3. Yang W, Lee TS (1995) J Chem Phys 103:5674
4. Lee TS, York DM, Yang W (1996) J Chem Phys 105:2744
5. Seijo L, Barandiarán Z (1992) J Math Chem 10:41
6. Ordejón P, Drabold DA, Martin RM, Grumbac MP (1995) Phys Rev B 51:1456
7. Stewart JP (1996) Int J Quantum Chem. 58:133
8. Shukla A, Dolg M, Stoll H (1998) Phys Rev B 58:4325

9. Helgaker T, Larsen H, Olsen J, Jorgensen P (2000) Chem Phys Lett 327:397
10. Head-Gordon M, Shao Y, Saravanan C, White CA (2003) Mol Phys 101:37
11. Goedecker S (1999) Rev Mod Phys 71:1085
12. Ordejón P (2000) Phys Status Solidi B 217:335
13. Hoffmann R (1963) J Chem Phys 39:1397
14. Ordejón P, Artacho E, Soler JM (1996) Phys Rev B 53:10441
15. Soler JM, Artacho E, Gale JD, García A, Junquera J, Ordejón P, Sánchez-Portal D (2002) J Phys Condens Matter 14:2745
16. Boys SF (1960) Rev Mod Phys 32:296
17. Edmiston C, Ruedenberg K (1963) Rev Mod Phys 35:457
18. Pipek J, Mezey PG (1989) J Chem Phys 90:4916
19. Ruedenberg K, Schmidt MW, Gilbert MM (1982) Chem Phys 71:51
20. Troullier N, Martins JL (1991) Phys Rev B 43:1993
21. Kleinman L, Bylander DM (1982) Phys Rev Lett 48:1425
22. Sankey OF, Niklewski DJ (1989) Phys Rev B 40:3979
23. Ordejón P, Drabold DA, Martin RM, Itoh S (1995) Phys Rev Lett 75:1394
24. Fernández-Serra MV, Artacho E (2004) J Chem Phys 121:11136